atmosphere

MDPI

Article

Minimizing contamination from plastic labware in the quantification of C16 and C18 fatty acids in filter samples of atmospheric particulate matter and their utility in apportioning cooking source contribution to urban $PM_{2.5}$

Yuk Ying Cheng[1], Jian Zhen Yu [1,2,3]*

[1] Department of Chemistry, Hong Kong University of Science & Technology, Clear Water Bay, Hong Kong, China
[2] Division of Environment & Sustainability, Hong Kong University of Science & Technology, Clear Water Bay, Hong Kong, China
[3] Guangdong-Hongkong-Macau Joint Laboratory of Collaborative Innovation for Environmental Quality, Hong Kong University of Science & Technology, Clear Water Bay, Hong Kong, China
* Correspondence: jian.yu@ust.hk, Tel: 852-2358-7389, Fax: 852-2358-1594

Received: 18 August 2020; Accepted: 14 October 2020; Published: date

Keywords: aerosol; organic aerosol; cooking aerosol; organic source tracers; tracer analysis; positive matrix factor analysis

---

Supplementary Materials

Additional information on positive matrix factorization (PMF) analysis

The full list of input species for the PMF analysis is provided in Table S1. Among them cholesterol was noted to have significantly elevated concentration in the P3 time segment (16:00-21:00), as seen in the time series plot (Figure S1). This feature reflects its cooking source emission characteristic, as dinner time falls in the P3 time segment. To adequately capture and model the higher cholesterol data during P3, we found using a varying error function (EF), a previously established technique (Wang et al., 2017), would be effective, and the details have been given in the main text. Figures S2(a)-S2(c) show the correlation matrix of select input species for the combined YL and MK dataset, the YL dataset, and the MK data set, respectively, to provide visual inspection and quantitative indication of correlation relationships between pairs of input species.

During our positive matrix factorization (PMF) analysis, settings for input species uncertainties and species category in term of "strong" or "weak" were determined by examining the interpretability of the resolved source profiles and how well the model-predicted concentrations compare with the measured ones. In the initial base run, the EF values for all species adopted fixed values; all input species with signal to noise ratios above 1 were set as "strong", except chloride ion (Cl^-) for the known influence from Cl^- depletion and OC was set as total variable. The resulting PMF solution, denoted as $PMF_{Chollinear}$ (Figure S3), was unable to resolve a clear cooking emission factor. Two factors (factors 6 and 7)) have signatures from both vehicular emissions and cooking emissions, as indicated by high loadings of hopanes and cholesterol, while factor 6 has a high loading of EC, indicating its stronger association with vehicular emissions. The modeled cholesterol by $PMF_{Chollinear}$ aligned better with the observed hopanes concentration (Figure S1), reflecting the mixing issue. The mixing of the two sources likely originated from some extent of co-varying emissions of vehicular and cooking sources, especially at the MK site, as indicated by the correlations between hopanes and cholesterol (Figure S2).

The issue in properly resolving cooking emission source was resolved by setting alkanes and K^+ ion as "weak" as they both could contribute from multiple emission sources/factors in PMF. The species category settings and constrains for the final PMF model are listed in Table S1. Figures S3-S5 are the source profiles resolved from different PMF runs. Figures S6 compares the modeled and observed values for $PM_{2.5}$, OC, and the three cooking tracers. Figure S7 shows the factor source contributions for individual samples at YL and MK.

Table S1. Summary of input species in final PMF model.

Species included	Group name	Category/ constrain type	Fixed EF	Major sources
OC		Total variable		Combustion sources and SOA formation
EC		Strong		Diesel trucks
Cl-		Weak		Sea salt
SO_4^{2-}		Strong		Secondary formation
NO^{3-}		Strong		
NH_4^+		Strong		
Na^+		Strong		Sea salt
K^+		Weak/pull down maximally in secondary factors & pull up maximally in biomass burning		Combustion sources
Cholesterol		Strong/ set to 0 in vehicular emission		Cooking
Palmitic acid		Strong/set to 0 in secondary sulfate factor		Cooking
Stearic acid				
benzo[b+k]fluoranthene, benzo[e]pyrene	PAHs252	Strong	0.4	Combustion sources
indeno[1,2,3-cd]pyrene, benzo[ghi]perylene	PAHs276	Strong	0.4	
αβ-norhopane (abH29)		Strong / set to 0 in SOA & cooking & biomass burning factors	0.3	Gasoline vehicles
αβ-hopane (abH30)			0.3	Gasoline vehicles
n-C_{29}, n-C_{31}, n-C_{33} alkane	Odd_Alk	Weak	0.3	Combustion sources or biogenic material
n-C_{28}, n-C_{30}, n-C_{32} alkane	Even_Alk	Weak	0.3	
Levoglucosan		Strong / pull up maximally in biomass burning factor	0.3	Biomass burning
Mannosan			0.4	
Vanillic acid			0.4	
2-methylthreitol, 2-methylerythritol	2-MTs	Strong	0.4	Isoprene-derived SOA
cis-2-methyl-1,3,4-trihydroxy-1-butene, 3-methyl-2,3,4-trihydroxy-1-butene, trans-2-methyl-1,3,4-trihydroxy-1-butene	C_5-alkene triols	Strong	0.4	
Pinic acid, 3-hydroxyglutaric acid	α-PinT	Strong	0.4	α-Pinene-derived SOA
β-caryophyllinic acid (β-cary acid)		Strong	0.4	β-caryophyllene-derived SOA
2,3-dihydroxy-4-oxopentanoic acid (2,3-DHOPA)		Strong	0.4	Toluene-derived SOA
Phthalic acid		Strong	0.4	Naphthalene-derived SOA

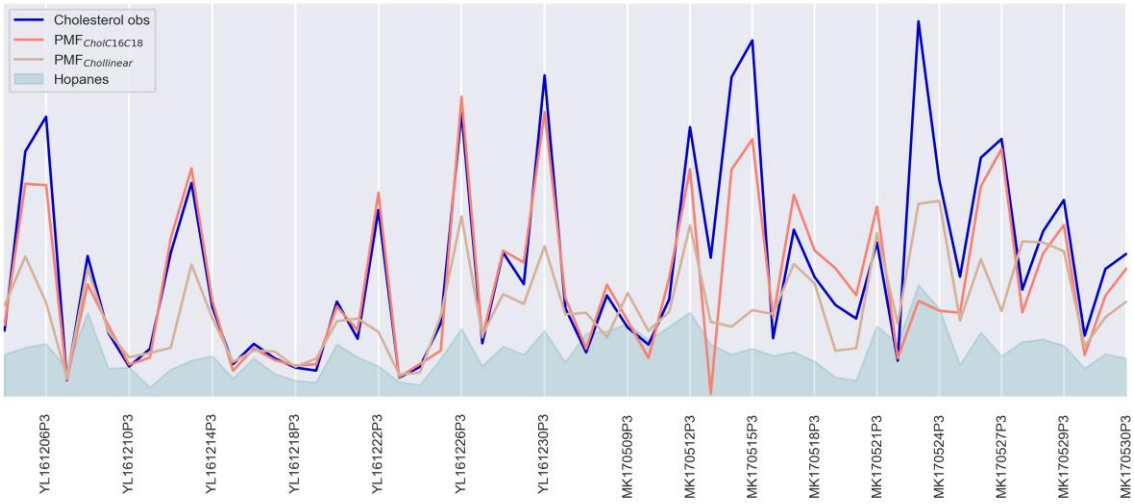

Figure S1. Time series of measured and modelled cholesterol concentrations. The modeled concentrations are from two PMF solutions, one with fixed EF (PMF$_{Chollinear}$, solid khaki line) and the second with a varying EF for cholesterol (PMF$_{CholC16C18}$, solid coral line). The observed hopane concentrations (teal shadow) are also shown to illustrate the variation of vehicular emissions. All the data share the same x and y axis.

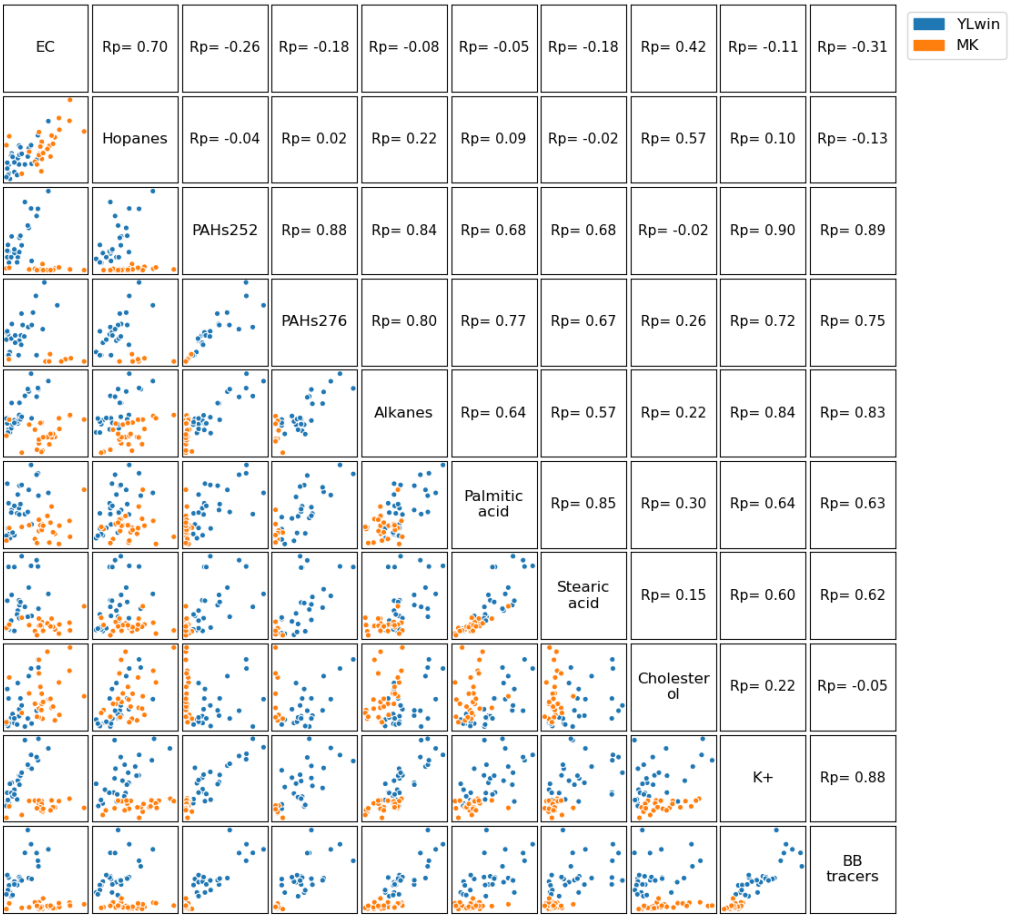

Figure S2(a). Correlation matrix of selected input species including 2 data sets, YL winter data in blue and MK data in orange. "Hopanes" is the concentration sum of abH29 and abH30, "Alkanes" is the sum of even and odd alkanes, and "BB tracers" is the sum of vanillic acid, mannosan and levoglucosan. The plots in the lower corner are the concentration scatter data, with YL winter marked in blue and MK in orange. The upper corner displays the Pearson's correlation coefficients (Rp).

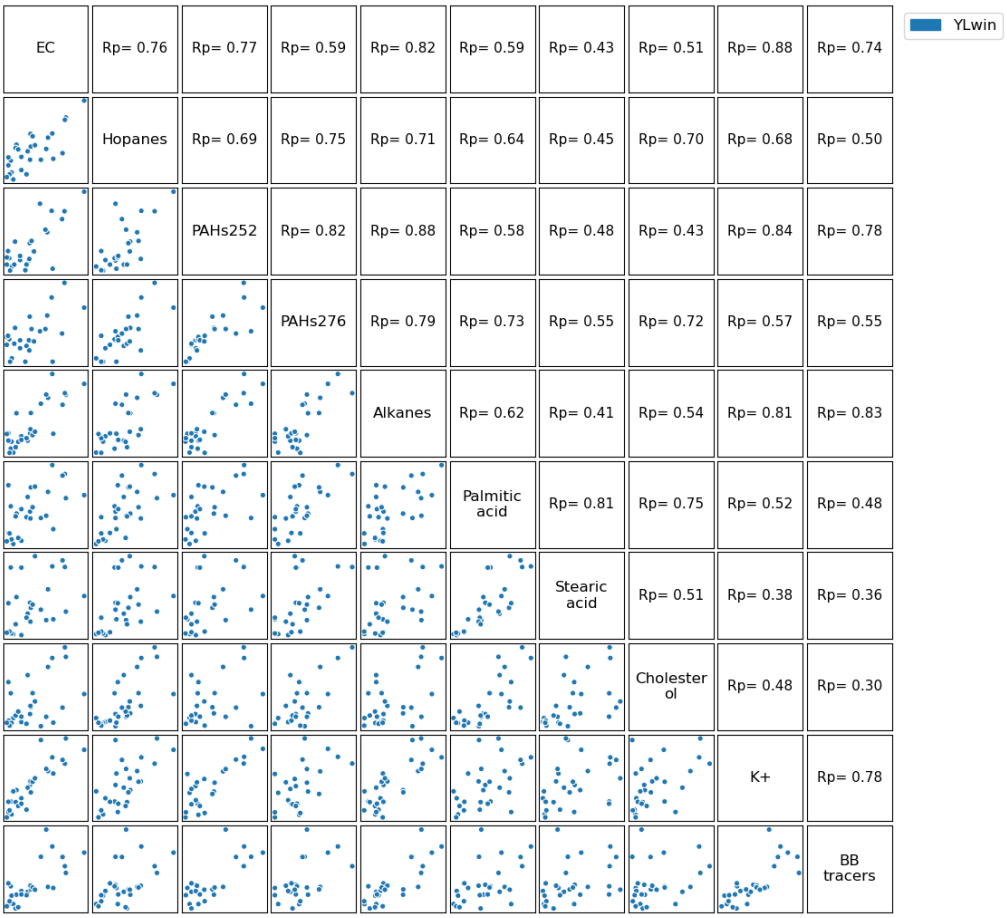

Figure S2(b). Correlation matrix of selected input species including YL winter data only. "Hopanes" was the concentration sum of abH29 and abH30. "Alkanes" was the concentration sum of even and odd alkanes. "BB tracers" was the concentration sum of vanillic acid, mannosan and levoglucosan. Lower corner of the plot was the concentration scatter matrix. Upper corner of the plot was the Pearson's correlation coefficients (Rp).

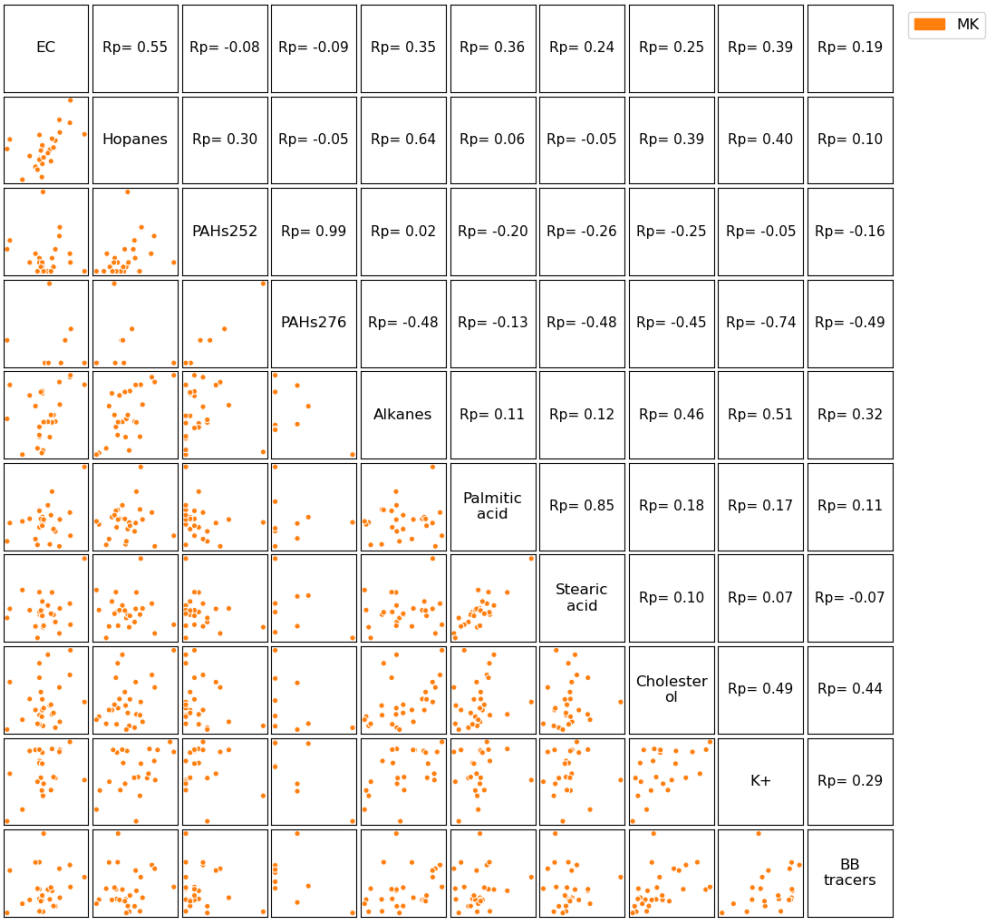

Figure S2(c). Correlation matrix of selected input species including MK data only. "Hopanes" was the concentration sum of abH29 and abH30. "Alkanes" was the concentration sum of even and odd alkanes. "BB tracers" was the concentration sum of vanillic acid, mannosan and levoglucosan. Lower corner of the plot was the concentration scatter matrix. Upper corner of the plot was the Pearson's correlation coefficients (Rp).

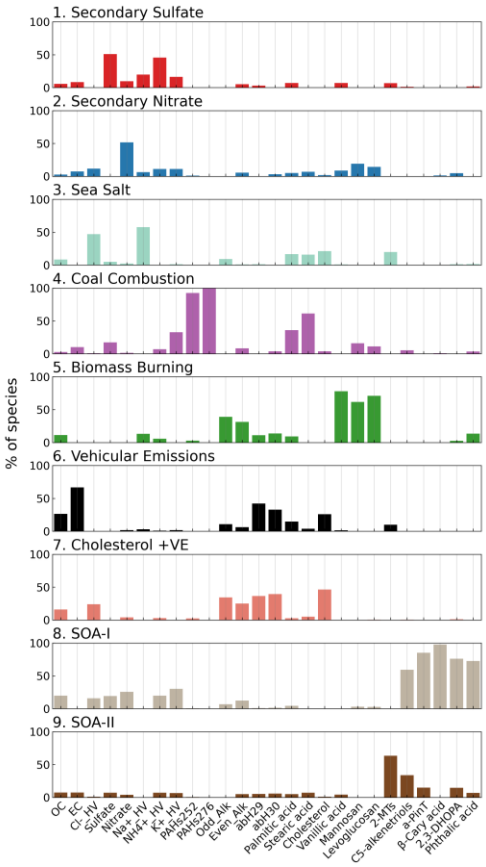

Figure S3. Prerun base factor profile ($PMF_{Chollinear}$) with fixed Error Fraction (EF) and set all other species as "Strong" except chloride ion as "Weak" and OC as total variable species. Cholesterol + VE denote as cholesterol mixed with vehicular emissions.

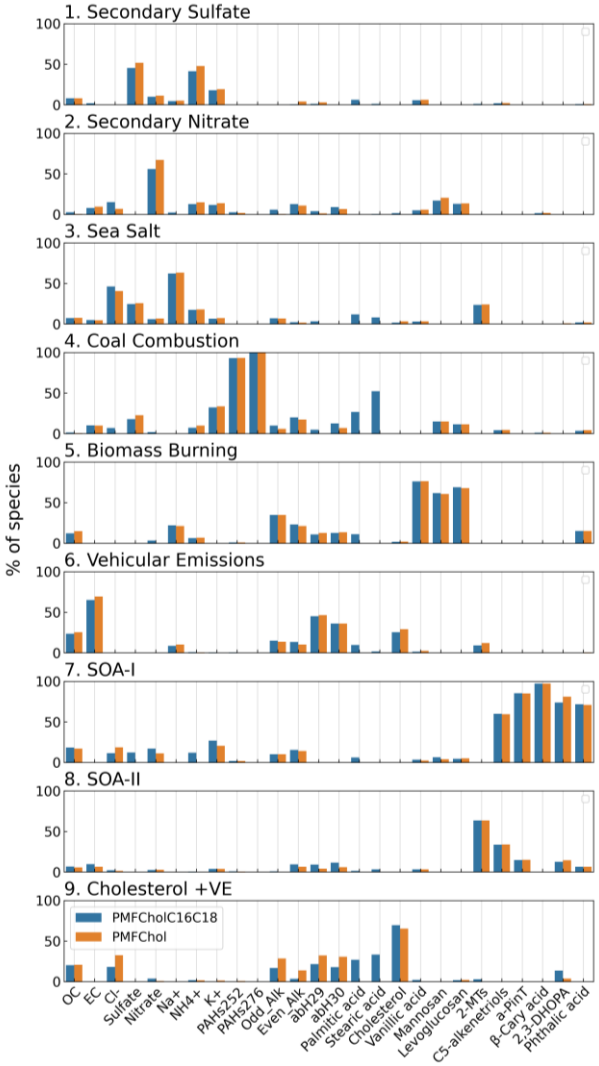

Figure S4. Comparison of source profiles resolved by the $PMF_{CholC16C18}$ base run and PMF_{Chol} base run with varying EF applied to both Cholesterol (a=0.1). The two PMF runs differ in whether fatty acids are included ($PMF_{CholC16C18}$) or excluded (PMF_{Chol}) as input species.

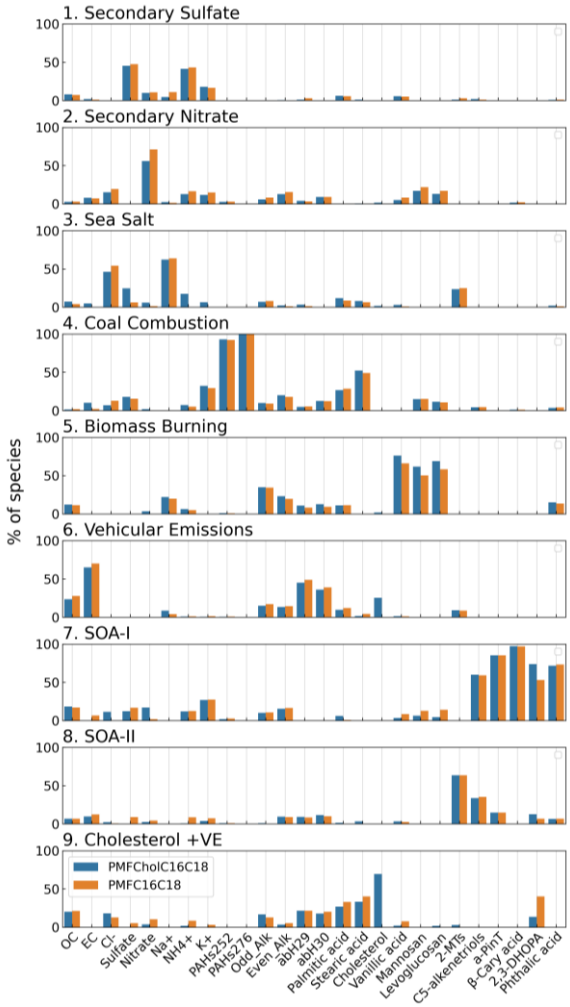

Figure S5. Comparison of source profiles resolved by the $PMF_{CholC16C18}$ base run and PMF_{C16C18} base run with varying EF applied to both Cholesterol (a=0.1). The two PMF runs differ in whether cholesterol is included ($PMF_{CholC16C18}$) or excluded (PMF_{C16C18}) as input species.

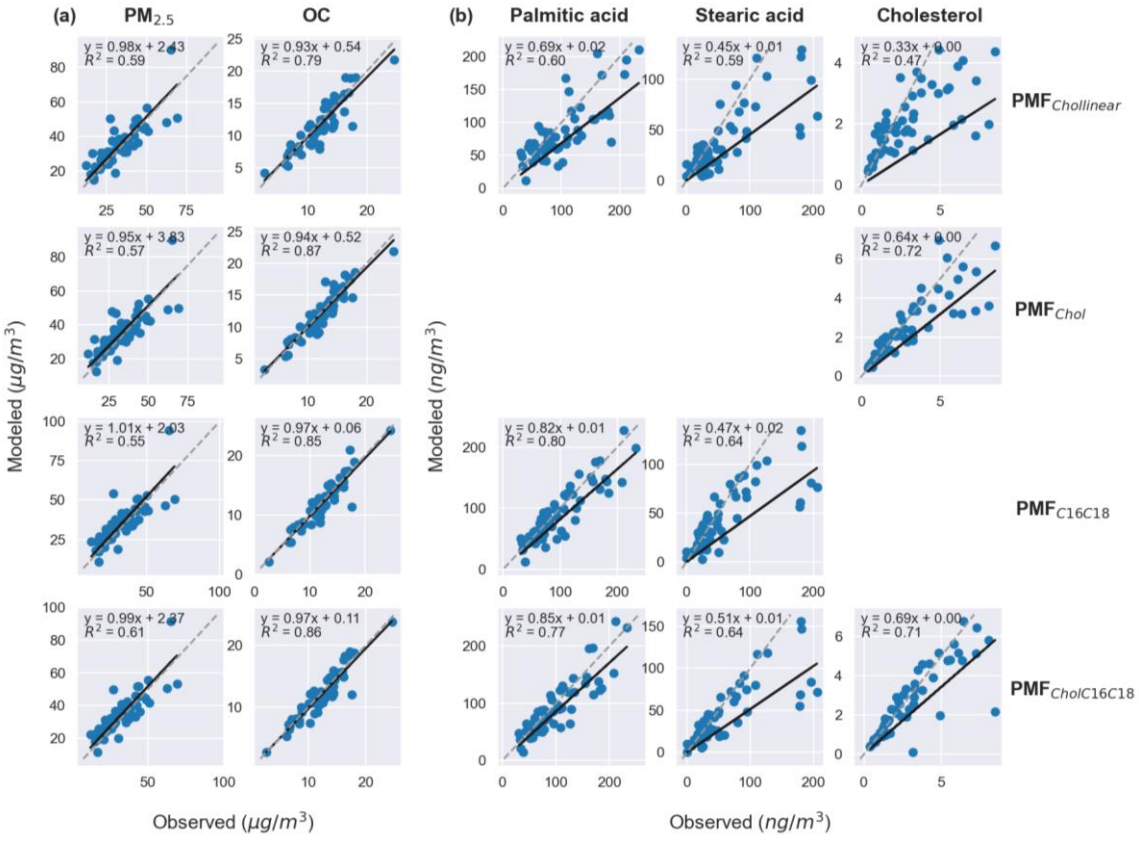

Figure S6. Scatter plots of modeled against observed data for (a) PM2.5 and OC and (b) the three cooking tracers (palmitic acid, stearic acid, and cholesterol). Four PMF solutions are included. $PMF_{Chollinear}$ in which a fixed EF is applied to cholesterol, PMF_{Chol} refers to the PMF run including cholesterol with varying EF (a=0.1) but excluding fatty acids as inputs, and $PMF_{CholC16C18}$ refers to the PMF run with all cooking tracers (cholesterol, palmitic acid and stearic acid) included. The solid line represents the regression equations generated by orthogonal distance regression and the dashed line is one-to-one line.

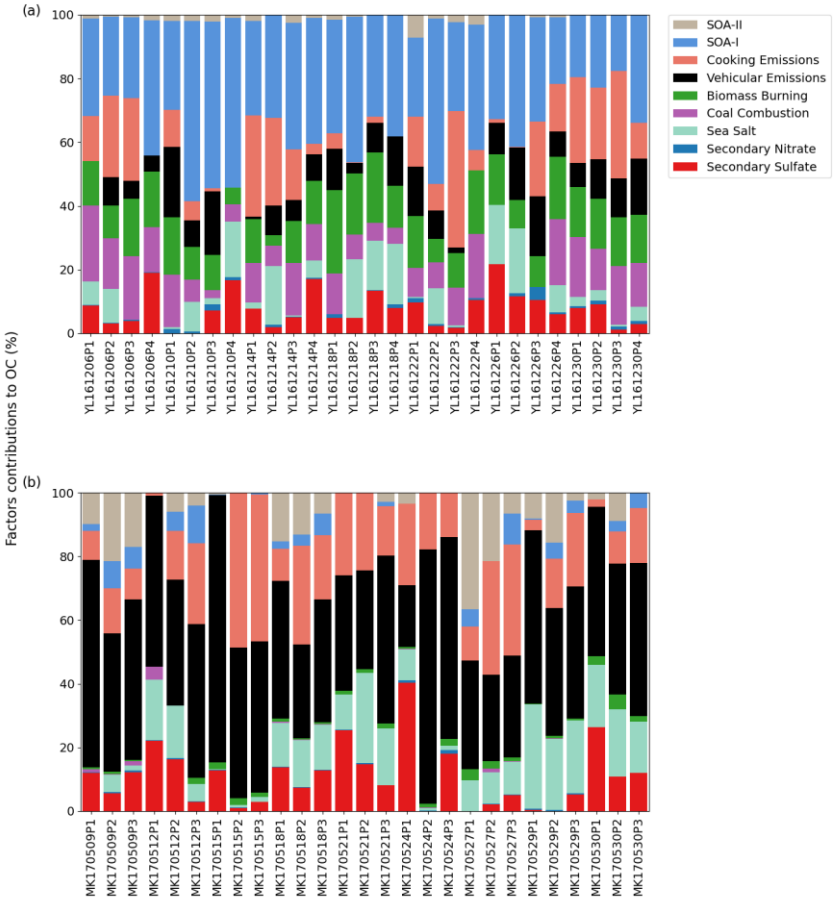

Figure S7. Factor source contributions to OC (%) from $PMF_{CholC16C18}$ for individual samples, (a) YL winter data (b) MK summer data.

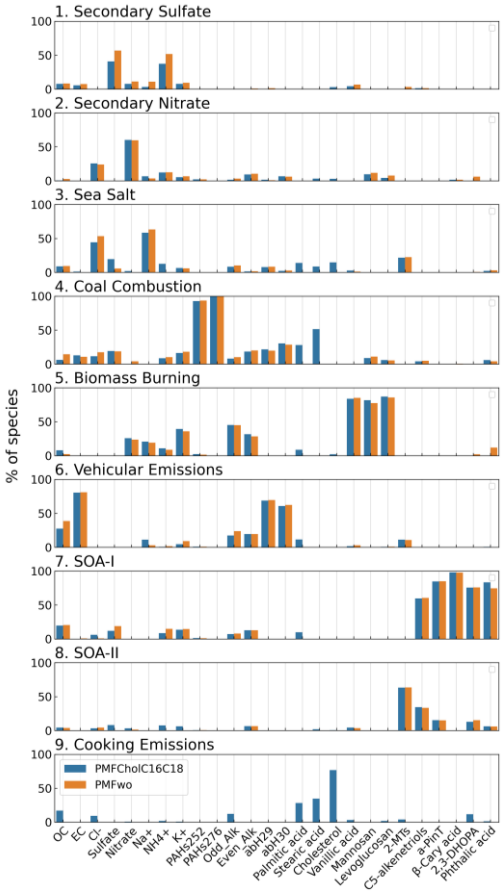

Figure S8. Comparison of source profiles resolved by the $PMF_{CholC16C18}$ and PMF_{wo} constrained runs. The two PMF runs differ in whether the three cooking tracers (palmitic acid, stearic acid and cholesterol) were included.

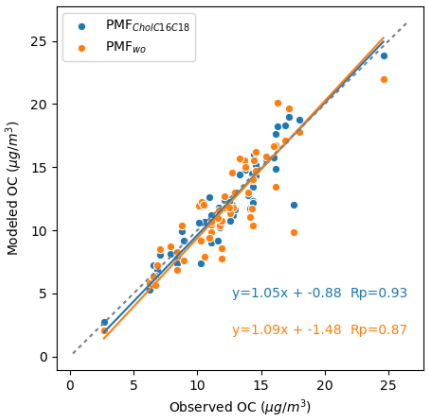

Figure S9. Scatter plots of modeled against observed OC data from $PMF_{CholC16C18}$ and PMF_{wo}. $PMF_{CholC16C18}$ refers to the PMF run with all cooking tracers (cholesterol, palmitic acid and stearic acid) included. PMF_{wo} refers to the PMF run without cooking tracers included. The solid line represents the regression equations generated by orthogonal distance regression and the dashed line is one-to-one line.